

## **SUPPLEMENTARY INFORMATION**

### **Native Kinesin-1 Does Not Bind Preferentially to GTP-Tubulin-Rich Microtubules In Vitro**

Qiaochu Li<sup>1</sup>, Stephen J. King<sup>2</sup>, and Jing Xu<sup>1,\*</sup>

<sup>1</sup>Department of Physics, University of California, Merced, CA 95343, USA

<sup>2</sup>Burnett School of Biomedical Sciences, University of Central Florida, FL 32827, USA

**\*Address correspondence to:** Jing Xu, E-mail: [jxu8@ucmerced.edu](mailto:jxu8@ucmerced.edu)

## SUPPORTING TEXT

### **GMPCPP microtubules do not require taxol to remain stable at room temperature**

We polymerized microtubules in the presence of GMPCPP to mimic GTP-tubulin-rich microtubules [Hyman et al., 1992; Nakata et al., 2011]. Importantly, we limited the concentration of tubulin to 4  $\mu\text{M}$  (Materials and Methods). This limited tubulin concentration is sufficient for the nucleation of microtubules in the presence of GMPCPP [Hyman et al., 1992] but not in the presence of GTP [Wieczorek et al., 2015].

We examined the stability of our GMPCPP microtubules in the absence of stabilizing agents (Fig. S2). In addition to trapping tubulin in a GTP-like state, GMPCPP also promotes the stability of polymerized microtubules: GMPCPP microtubules depolymerize  $\sim 5000\times$  more slowly than GDP microtubules ( $0.1 \text{ s}^{-1}$  vs.  $500 \text{ s}^{-1}$ , respectively; [Hyman et al., 1992]).

We first examined the short-term stability of our GMPCPP microtubules. Briefly, fluorescently labeled microtubules were polymerized at 37  $^{\circ}\text{C}$ , diluted to 40 nM in PEM buffer (warmed to 37  $^{\circ}\text{C}$ ), and imaged at room temperature within 10 min of dilution (Materials and Methods). While GMPCPP microtubules remained intact in the absence of stabilizing agents, under otherwise identical conditions, GDP microtubules remained intact only in the presence of the stabilizing agent taxol (Fig. S2A). This stability difference between microtubule types indicates that GMPCPP was successfully incorporated into our GMPCPP microtubules.

We next quantified the long-term stability of our GMPCPP microtubules (Fig. S2B-D). After polymerization, GMPCPP microtubules (4  $\mu\text{M}$ ) were placed in a dark box at room temperature without stabilizing agents, and microtubule length was quantified as a function of

time elapsed. Although we predicted that depolymerization would significantly reduce microtubule length, we did not detect such a reduction (Fig. S2B-D). Instead, we uncovered a significant 2.6x increase in the length of microtubules over 80 h (3.2  $\mu\text{m}$  at 0.5 h vs. 8.4  $\mu\text{m}$  at 80 h, Fig. S2B-D;  $P = 8 \times 10^{-7}$ , rank-sum test). Note that this length increase likely includes some degree of end-to-end annealing of microtubules, as previously demonstrated by others [Caplow et al., 1986; Rothwell et al., 1986] and ourselves [Gramlich et al., 2017]. Regardless of the specific mechanism, this length increase establishes that taxol-free GMPCPP microtubules do not undergo substantial depolymerization, in contrast to GDP microtubules.

Taken together, the data in Figure S2 demonstrate that GMPCPP microtubules are distinct from GDP microtubules, and are appropriate for investigating the role of tubulin-nucleotide state on multiple-kinesin transport.

## SUPPORTING FIGURES

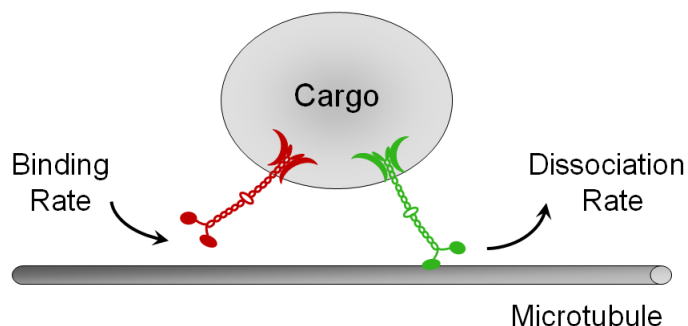


**Figure S1. The run length of multiple-motor cargos is sensitive to both the binding and dissociation rates of individual motors for the microtubule.** The illustration is not to scale. For simplicity, we depict two representative motors during cargo transport. During transport, the bound motor (green) can dissociate from the microtubule. The greater the dissociation rate, the smaller the number of motors linking the cargo to the microtubule, and the shorter the cargo's run length. At the same time, an unbound motor (red) can bind the microtubule and engage in transport. The greater the motor's binding rate, the faster the unbound motor rebinds the microtubule. This effect increases the net number of motors linking the cargo to the microtubule at any time, thereby increasing the overall run length of the cargo. Previous reports indicate a substantially higher (3.7x) binding affinity of kinesin-1 for GMPCPP microtubules versus GDP microtubules [Nakata et al., 2011]. In the current study, we examined the implication of such an increase in kinesin's binding affinity for the run length of multiple-kinesin cargos.

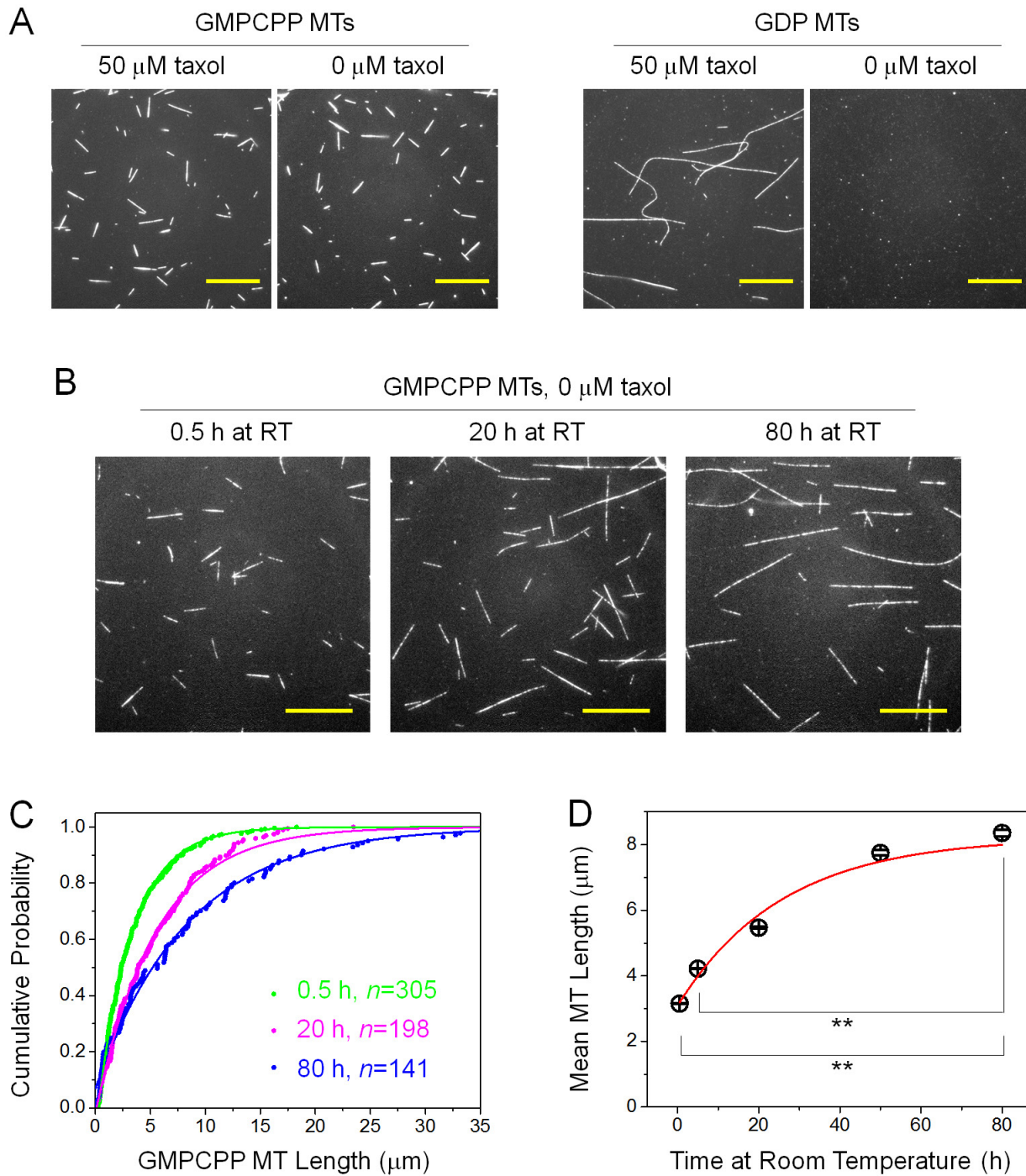


**Figure S2. GMPCPP microtubules (MTs) are stable at room temperature without the stabilizing agent taxol.** (A) Representative fluorescence images of GMPCPP MTs and GDP MTs in the absence and in the presence of taxol. MTs for each condition were imaged within 10

min of being moved from a 37 °C water bath to room temperature (RT). Scale bar, 20 μm. (B) Representative fluorescence images of taxol-free GMPCPP MTs that were kept at RT for the indicated time in the absence of taxol. Scale bar, 20 μm. (C) Cumulative probability distributions of MT lengths corresponding to conditions in (B).  $n$ , sample size. Solid lines, best fits to  $1-Ae^{-x/L}$ , where  $L$  is the mean MT length. (D) Mean length of taxol-free GMPCPP MTs (scatters ± standard error) as a function of the time kept at RT. Red line, exponential growth trend.  $**P \leq 0.022$ , rank-sum test.

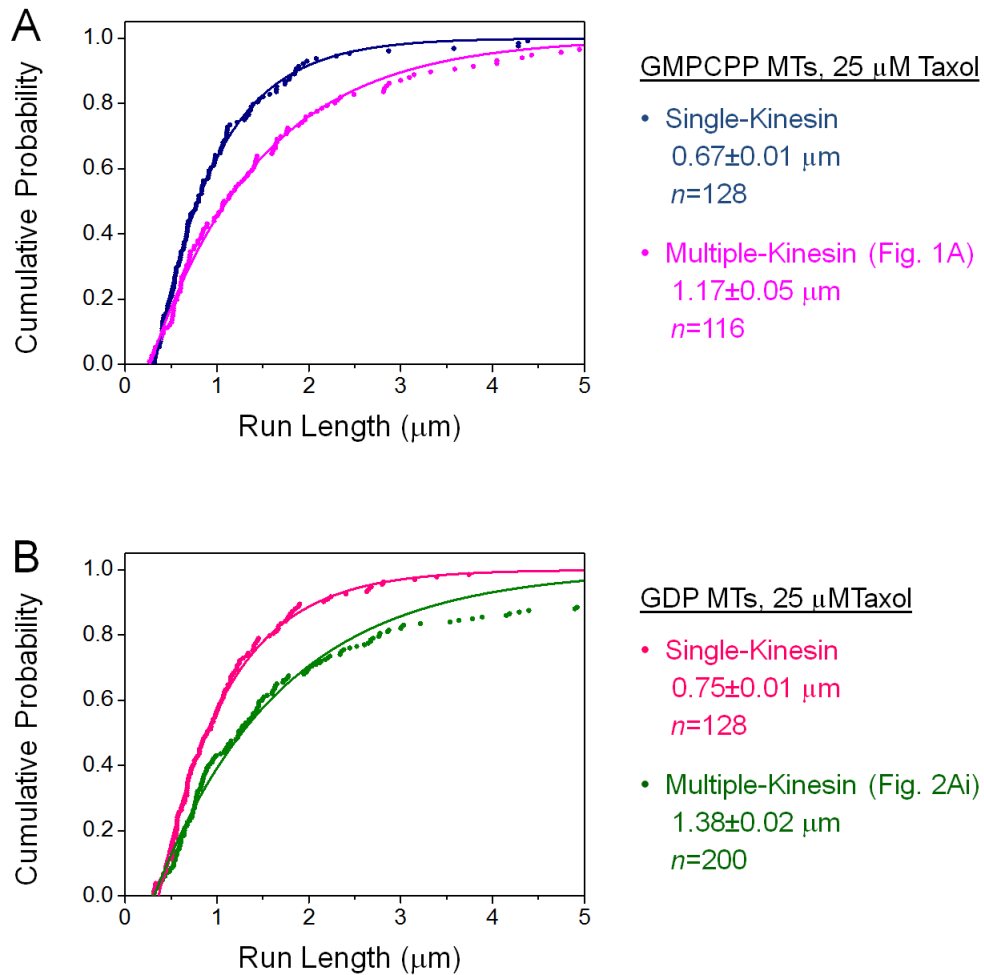


**Figure S3. A  $\sim 1.7\times$  increase in run length versus the single-kinesin value indicates that cargo transport was driven by  $\sim$ two kinesins.** Taxol (25  $\mu\text{M}$ ) was present in buffers during motility experiments for both microtubule (MT) types. Solid lines, best fits to  $1-Ae^{-x/d}$ , where  $d$  is the mean run length. (A) Cumulative probability distribution for single-kinesin cargos versus multiple-kinesin cargos along GMPCPP MTs. Mean run length ( $\pm$  standard error) and sample size ( $n$ ) are indicated. These distributions differ from each other significantly ( $P = 0.002$ , rank-

sum test). (B) Cumulative probability distribution for single-kinesin cargos versus multiple-kinesin cargos along GDP MTs. Mean run length ( $\pm$  standard error) and sample size ( $n$ ) are indicated. These distributions differ from each other significantly ( $P = 0.0001$ , rank-sum test).



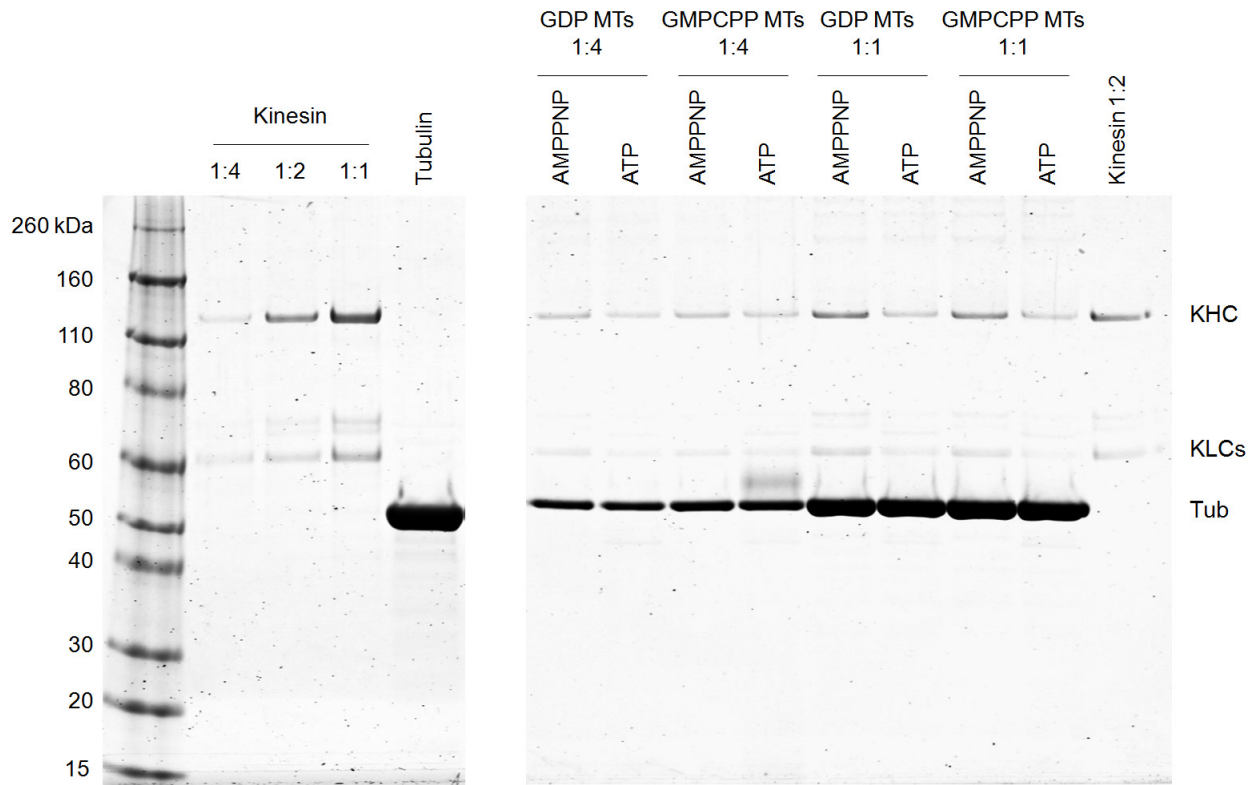


**Figure S4. Coomassie-stained gels of the proteins used in the current study (left) and of the microtubule pulldown assays corresponding to Figure 6A in the main text (right).** KHC, kinesin heavy chain; KLC, kinesin light chain; Tub, tubulin. (Left) Serial dilutions of kinesin reference solutions (1:1, 1:2, and 1:4) correspond to total protein content of 800 ng, 400 ng, and 200 ng per lane. Tubulin reference lane corresponds to a total protein content of 3  $\mu$ g. (Right) Example co-sedimentation assays at two microtubule concentrations (1:1 and 1:4, corresponding to 0.28 and 1.1  $\mu$ M MT, respectively), and in the presence of 5 mM AMPPNP or 5 mM ATP as indicated. Assays using GDP MTs contained taxol (25  $\mu$ M). Assays using GMPCPP MTs were free of taxol.

## **SUPPORTING REFERENCES**

Caplow, M., Shanks, J., and Brylawski, B.P. 1986. Differentiation between Dynamic Instability and End-to-End Annealing Models for Length Changes of Steady-State Microtubules. *Journal of Biological Chemistry* 261: 6233-6240.

Gramlich, M.W., Conway, L., Liang, W.H., Labastide, J.A., King, S.J., Xu, J., and Ross, J.L. 2017. Single Molecule Investigation of Kinesin-1 Motility Using Engineered Microtubule Defects. *Sci Rep* 7: 44290.

Hyman, A.A., Salser, S., Drechsel, D.N., Unwin, N., and Mitchison, T.J. 1992. Role of GTP hydrolysis in microtubule dynamics: information from a slowly hydrolyzable analogue, GMPCPP. *Mol Biol Cell* 3: 1155-1167.

Nakata, T., Niwa, S., Okada, Y., Perez, F., and Hirokawa, N. 2011. Preferential binding of a kinesin-1 motor to GTP-tubulin-rich microtubules underlies polarized vesicle transport. *J Cell Biol* 194: 245-255.

Rothwell, S.W., Grasser, W.A., and Murphy, D.B. 1986. End-to-end annealing of microtubules in vitro. *J Cell Biol* 102: 619-627.

Wieczorek, M., Bechstedt, S., Chaaban, S., and Brouhard, G.J. 2015. Microtubule-associated proteins control the kinetics of microtubule nucleation. *Nat Cell Biol* 17: 907-916.